

# Timing Acquisition for Pulse-based Wireless Systems in the Terahertz Band

Chong Han  
Broadband Wireless  
Networking Laboratory  
(BWN-Lab),  
Georgia Institute of  
Technology, Atlanta, USA  
chong.han@ece.gatech.edu

Ian F. Akyildiz  
Broadband Wireless  
Networking Laboratory  
(BWN-Lab),  
Georgia Institute of  
Technology, Atlanta, USA  
ian@ece.gatech.edu

Wolfgang H. Gerstacker  
Institute for Digital  
Communications,  
Friedrich-Alexander-University  
Erlangen-Nürnberg (FAU),  
Erlangen, Germany  
gersta@LNT.de

## ABSTRACT

Terahertz (0.06-10 THz) band communication is envisioned as a key technology to satisfy the increasing demand for ultra-broadband wireless communication. Due to the very broad bandwidth and high frequency-selectivity, the synchronization faces major challenges, such as the ultra-high sampling rate demand, the stringent timing requirement for demodulation, and the THz band communication peculiarities. To address these challenges, in this paper, two algorithms for timing acquisition are proposed. First, a low-sampling-rate (LSR) synchronization algorithm is developed, by extending the theory of sampling signals with finite rate of innovation in the communication context and exploiting the annihilating filter method. Moreover, a maximum likelihood (ML)-based approach for timing acquisition is developed, which is a two-step procedure and uses the weighted average template construction to exploit the ML criterion. Extensive simulations are carried out, and the results show that the LSR algorithm is desired with the uniform sampling at  $1/20$  of the Nyquist rate for the directional transmission, while the ML-based algorithm is suitable in the multipath propagation with a half-reduced searching space.

## Keywords

Terahertz Band, Timing Acquisition, Synchronization

## 1. INTRODUCTION

In recent years, the wireless data traffic grew exponentially, further accompanied by an increasing demand for higher data rates [11]. New spectral bands as well as advanced physical layer solutions are required to support this high data rate for future wireless communications. In addition to many proposed solutions for next generation advanced cellular systems, the (0.06 - 10) Terahertz band is identified as one of the promising spectrum bands to enable

ultra-high-speed communications [2]. Synchronization provides accurate timing information of the received signal to accomplish demodulation at the receiver, and it becomes a challenging problem in ultra-high-speed wireless communication networks in the THz band. Timing errors as small as picoseconds can seriously degrade the system performance. The unique challenges and requirements for the THz band synchronization are as follows.

First, *demand of ultra-high sampling rates*. A clear trend for system design is to perform as much digital processing as possible, since digital implementation has the advantages of cost-efficiency, full integration, and robustness [9]. Given the very broad bandwidth of the THz band signaling (ranging from tens of GHz up to several THz [4]), the digital synchronization requires extremely fast sampling, expensive and high power consuming analog-to-digital converters, operating at multi-GHz and even THz. Second, *stringent timing requirement for demodulation*. The ultra-short pulses employed in THz band systems place stringent timing requirements for demodulation. For the time being, the feasibility of carrier-based modulation is limited by the lack of compact transceivers that are able to generate THz carrier frequencies. Recently in [6], the ultra-short pulse-based modulation is proposed to capture the expected capabilities of THz signal generators and detectors. The very broad bandwidth results in an ultra-fine resolution of the timing uncertainty region and imposes a very large search space for detection-based synchronization approaches [1]. Lastly, *THz band communication and propagation peculiarities*. The THz band channel is highly frequency-selective, and has severe attenuation as well as distortion on the transmitted pulses [5]. The severe frequency-selectivity causes temporal broadening on the transmitted signals and hence, increases the burden of timing acquisition. Furthermore, the high-gain antennas and very large antenna arrays are suggested in [2] to overcome the very high path loss, which can effectively reduce the multipath effects. Therefore, the THz band transmission can be either multipath with a low number of the total paths or directional in the extreme case.

To address these challenges above, in this paper, we develop a *low-sampling-rate (LSR) algorithm* for timing acquisition, which extends the theory of sampling signals with *finite rate of innovation* in the communication context and exploits the features of *annihilating filters* [12]. According to the classical sampling theory [3], the very broad signal bandwidth prescribes a prohibitively high sampling rate and

Permission to make digital or hard copies of all or part of this work for personal or classroom use is granted without fee provided that copies are not made or distributed for profit or commercial advantage and that copies bear this notice and the full citation on the first page. To copy otherwise, to republish, to post on servers or to redistribute to lists, requires prior specific permission and/or a fee.

NANOCOM'15, September 21 - 22, 2015, Boston, MA, USA

Copyright 2015 ACM 978-1-4503-3674-1/15/09 ...\$15.00.

DOI: <http://dx.doi.org/10.1145/2800795.2800819>.

digital synchronization becomes very expensive. However, a signal that is not bandlimited can still be completely reconstructed from uniform samples, provided that the signal has a finite rate of innovation, as proved in [10, 8]. In the communication context, the rate of innovation refers to the symbol rate. Therefore, we develop the LSR synchronization algorithm that samples faster than the symbol rate, but at a fraction of the sampling rate dictated by the signal bandwidth, i.e., the Nyquist rate.

In addition to the LSR algorithm, we propose a *maximum-likelihood* (ML)-based approach for timing acquisition. In particular, a two-step procedure and the weighted average template construction are used in the process to derive the timing acquisition solutions based on the ML criterion. We perform extensive performance evaluation on the developed two algorithm via simulations. We investigate the impact of different communication parameters on the acquisition performance and compare the two algorithms. Our paper contributes to synchronization design with reduced computation complexity and efficient timing acquisition for the THz band systems.

The rest of this paper is organized as follows. In Section 2, we analyze the channel and the signal model for THz band communication. We proceed to delineate LSR synchronization algorithm in Section 3. Moreover, the timing acquisition solutions based on the ML criterion is derived in Section 4. Extensive simulations and performance evaluation are presented in Section 5. Finally, we conclude the paper in Section 6.

## 2. TERAHERTZ BAND CHANNEL AND WAVEFORM MODEL

In this section, we introduce the propagation model in the THz band. Based on the channel model, we describe the pulse-based THz signal model and derived the signals at the receiver in the time and frequency domains. Furthermore, we define the timing acquisition problem associated with the THz signaling.

### 2.1 Overview of Terahertz Band Channel

The complete multipath channel model in the THz band has been introduced in our previous study [4]. In this section, we present the directional transmission model, as an extension of the free space model in [5]. In particular, we consider the channel frequency response in the THz band consisting of the spreading loss, the molecular absorption loss, and the reflection loss, as

$$H(f) = G_t G_r \cdot \frac{c}{4\pi f d_T} \cdot \exp\left(-\frac{1}{2}\mathcal{K}(f)d_T\right) \cdot \mathcal{R}(f) \quad (1)$$

where  $G_t$  and  $G_r$  denote the transmit and receive antenna gains. Moreover,  $c$  stands for the speed of light,  $f$  is the operating frequency, and  $d_T$  represents the total traveling distance. The *molecular absorption coefficient*  $\mathcal{K}$  is frequency-selective and computed in [5]. The reflection coefficient for a rough surface,  $\mathcal{R}$ , is computed as

$$\mathcal{R}(f) = \begin{cases} 1, & \text{LoS} \\ \frac{\cos(\theta) - n_t \sqrt{1 - \left(\frac{1}{n_t} \sin(\theta)\right)^2}}{\cos(\theta) + n_t \sqrt{1 - \left(\frac{1}{n_t} \sin(\theta)\right)^2}} e^{-\frac{8\pi^2 f^2 \sigma_R^2 \cos^2(\theta)}{c^2}}, & \text{NLoS} \end{cases}, \quad (2)$$

On the one hand, there is no reflection loss for LoS.  $d_T$  is equal to the direct distance  $d$  if LoS is present. On the other hand, in the directed NLoS mode, the refractive index,  $n_t$ , is a function of the operating frequency and the reflection material. If we denote  $\theta$  as the incident angle of the reflected path,  $d_T = d/\cos(\theta)$ . Furthermore,  $\sigma_R$  is the factor that characterizes the roughness of the reflecting surface.

### 2.2 Terahertz Pulse Waveform

In [6], the wideband pulse waveform is proposed for the purposes of ultra-low power, compact-size and ultra-low complexity design for THz band communication. The pulse width is  $T_p$ . Every information symbol consists of a block of these repeated pulses (one pulse per frame), and the resulting transmitted signal is shown in Fig. 1 and is

$$s(t) = \sum_{i=0}^{I-1} a_i \sum_{k=0}^{N_f-1} p(t - iN_f T_f - kT_f - \tau_0), \quad (3)$$

where  $a_i$  refers to the  $i^{\text{th}}$  symbol taking values 0 or 1,  $p(t)$  is the transmission pulse. Moreover,  $N_f$  is the number of pulse waveforms to represent one symbol, which is also known as the number of frames.  $T_f$  stands for the separation between the consecutive pulses, and  $\tau_0$  represents the random initial transmission delay.  $I$  is the total number of symbols.

The time response of the THz band channel is obtained by using the inverse Fourier transform on (1)  $h(t) = \mathcal{F}^{-1}\{H(f)\}$ . The received signal after the channel is passed through a receiver filter  $h_R$ , and the filter output is

$$y(t) = \sum_{i=0}^{I-1} a_i \sum_{\mu_i, \nu_i}^{N_f-1} g(t - iN_f T_f - kT_f - \mu_i T_f - \nu_i T_s) + w(t) \quad (4)$$

$$\text{with} \quad g(t) = p(t) * h(t) * h_R(t), \quad (5)$$

$$\mu_i T_f + \nu_i T_s = \tau_0 + t_D + \psi_i. \quad (6)$$

In the above equations,  $w$  is the white Gaussian noise,  $t_D = d_T/c$  stands for the transmission delay, and  $\psi_i$  denotes the jittering offset or the random misalignment between the transmitter and receiver clocks, which dynamically varies over symbols. In (6),  $\mu_i$  identifies the first frame of a symbol, which amounts to the symbol timing (ST) at a frame level, and suggests that a symbol begins at  $t = iN_f T_f + \mu_i T_f$ . On the other hand,  $\nu_i$  indicates the frames' starting time, which is the frame timing (FT) at a sample level, and indicates a frame begins at  $t = (iN_f + k + \mu_i)T_f + \nu_i T_s$ , with  $T_s = 1/f_s$  being the sampling interval.

Consequently, the *timing acquisition* for the THz band communication includes: i) the random starting time,  $\tau_0$ , ii) the propagation delay,  $t_D$ , which is a constant if the transmitter and the receiver are fixed, and iii) the jittering offset,  $\psi_i$ , which is different for the different symbols. Equivalently, finding these parameters is related to solving for  $\mu_i$  and  $\nu_i$ .

By performing the Fourier Transform, the equivalent signal model in the frequency domain is expressed as

$$Y(f) = \sum_{i=0}^{I-1} a_i \sum_{k=0}^{N_f-1} G_t G_r \cdot \frac{c}{4\pi f d_T} \cdot \exp\left(-\frac{1}{2}\mathcal{K}(f)d_T\right) \cdot \mathcal{R}(f) P(f) H_R(f) \exp(-j2\pi f (iN_f T_f + kT_f)) \cdot \exp(-j2\pi f (\mu_i T_f + \nu_i T_s)) + W(f) \quad (7)$$

where  $P$ ,  $H_R$  and  $W$  represent the frequency responses of  $p$  and  $h_R$ , and  $w$ , in (4) and (5). Furthermore, we define a sampling interval  $T_s = T_f/Q$ , where  $Q$  is an integer that denotes the number of samples per frame. Hence,  $\nu_i$  takes values in the range of  $[0, Q - 1]$ , while the multiple of  $T_f$  is absorbed in  $\mu_i$ . After sampling at a sampling rate  $N_s$  with the time interval  $T_s$ , the discrete signal becomes

$$y[n] = \sum_{i=0}^{I-1} a_i \sum_{k=0}^{N_f-1} g[n - iN_fQ - kQ - \mu_iQ - \nu_i] + w[n]. \quad (8)$$

Next, we transform the signals into the frequency domain, and we consider the bandlimited filter has a center frequency  $f_c = \frac{f_U + f_L}{2}$ , where  $f_U$  and  $f_L$  denote the upper and lower cutoff frequencies of the filter. The sampling rate satisfies  $f_s = \frac{1}{T_s} \geq f_U - f_L$ . The frequency step is defined as  $f_0 = \frac{f_U - f_L}{N}$ . In the frequency domain, the total  $N$  uniformly spaced frequency samples can be expressed as

$$\begin{aligned} Y[n] &= \sum_{i=0}^{I-1} A_i[n] \sum_{k=0}^{N_f-1} \exp(-j2\pi f_n i N_f T_f + k T_f) \\ &\quad \cdot \exp(-j2\pi f_n \mu_i T_f + \nu_i T_s) + W[n] \\ &= \sum_{i=0}^{I-1} A_i[n] \sum_{k=0}^{N_f-1} \exp(-j2\pi f_n T_f (i N_f + k + \mu_i)) \\ &\quad \cdot \exp(-j2\pi f_n T_s \nu_i) + W[n] \\ &= \sum_{i=0}^{I-1} \sum_{k=0}^{N_f-1} A_i[n] u_i^n + W[n] \end{aligned} \quad (9)$$

where  $f_n = f_L + n f_0$ . In the above equations, the expanded expressions for  $A_i$  and  $u_i^n$  are given by

$$A_i(f) = a_i G_t G_r \cdot \frac{c}{4\pi f d_T} \cdot \exp\left(-\frac{1}{2} \mathcal{K}(f) d_T\right) \cdot \mathcal{R}(f) P(f) H_R(f), \quad (10)$$

$$u_i^n = e^{(-j2\pi f_n T_f (i N_f + k + \mu_i)) + (-j2\pi f_n T_s \nu_i)}. \quad (11)$$

By using a polynomial approximation to express the coefficients  $A_i[n]$ , with a sum of polynomials with degree  $0 \leq m \leq M - 1$ . Hence, the expression for  $Y[n]$  in (9) can be further approximated as

$$Y[n] \approx \sum_{i=0}^{I-1} \sum_{k=0}^{N_f-1} \left( \sum_{m=0}^{M-1} x_m n^m \right) u_i^n + W[n]. \quad (12)$$

This received signal will be used for the time acquisition, by using the LSR and the ML algorithms in the sequel sections.

### 3. LOW-SAMPLING-RATE (LSR) TIMING ACQUISITION ALGORITHM

A signal that is not bandlimited can still be completely reconstructed from uniform samples, provided that the signal has a finite rate of innovation, as proved in [8]. The key in constructions is to identify the innovative part of a signal. In the signal model in (12), the finite rate of innovation includes the parameters  $\epsilon_{\mu, \nu}$  and  $x_m$ . In this section, we present the LSR algorithm that captures the channel and communication peculiarities in the THz band. This algorithm is based on the annihilating filter method and the spectral estimation techniques in the frequency domain, and is useful to

estimate the timing information at a sub-Nyquist rate. In particular, the annihilating filter method is a well-known tool from spectral estimation or error correction coding [10], while in our context, we consider deterministic signals and derive the analytical sampling formulas.

The LSR algorithm for synchronization is given in Fig. 2. The *LSR factor* is defined as the ratio between the Nyquist sampling rate and the implemented sampling rate, as  $\beta_{\text{LSR}} = N_n/N_s$ . Based on the THz band channel in Sec. 2.1 and the pulse waveform in Sec. 2.2, we start with designing the annihilating filter,  $H_a[m]$ . The  $N$  spectral coefficients  $Y[n]$  are computed in (12), with  $N \geq 2L + 1$ . The annihilating filter is designed to allow

$$\begin{aligned} H_a[n] * Y[n] &= \sum_{l=0}^L H_a[l] Y[n - l] \\ &= 0, \text{ for } n = 0, 1, \dots, N, \end{aligned} \quad (13)$$

where  $L = I \cdot N_f \cdot M$ . In light of (12), the annihilating filter is in the form of

$$H_a(z) = \prod_{i=0}^{I-1} \prod_{k=0}^{N_f-1} [1 - p_{i,k}^0 z^{-1}]^M, \quad (14)$$

where  $p_{i,k}^0$  is a function of the frequency step  $f_0$  and relates to  $u_i^n$ , as

$$\begin{aligned} p_{i,k}^0 &= \exp(-j2\pi f_0 T_f (i N_f + k + \mu_i) - j2\pi f_0 T_s \nu_i) \\ &= (u_i^n \cdot \exp(j2\pi f_L (T_f (i N_f + k + \mu_i) + T_s \nu_i)))^{\frac{1}{n}}. \end{aligned} \quad (15)$$

The proof of this annihilating filter is omitted. The annihilating filter has the degree of  $L$ , and in this equation, there are  $L + 1$  unknown filter coefficients, which require  $L + 1$  linear equations to solve for the annihilating filter coefficients. To efficiently solve for the annihilating filter coefficients, we can set  $H_a[0] = 1$ , without loss of generality. Then, the matrix equation can be arranged as  $\mathbf{Y}' \cdot \mathbf{H}'_a = -\mathbf{Y}_1$ , where the matrices are defined as

$$\mathbf{Y}' = \begin{pmatrix} Y[L-1] & Y[L-2] & \dots & Y[0] \\ Y[L] & Y[L-1] & \dots & Y[1] \\ \vdots & \vdots & \ddots & \vdots \\ Y[2L-1] & Y[2L-2] & \dots & Y[L] \end{pmatrix}, \quad (16)$$

$$\mathbf{H}'_a = (H_a[1] \ H_a[2] \ \dots \ H_a[L])^T, \quad (17)$$

$$\mathbf{Y}_1 = (Y[L] \ Y[L+1] \ \dots \ Y[2L] \ \dots)^T, \quad (18)$$

where  $(\cdot)^T$  denotes the transpose operator.

Next, we utilize the derivations above to compute the timing offsets. With the filter coefficients  $H_a[m]$ , the values of  $\mu_i$  and  $\nu_i$  can be estimated by exploiting the pole properties of the annihilating filter. By transforming the annihilating filter into the  $z$ -domain, we relate the filter coefficients to the desired timing parameters and search for the roots that are closest to the unit circle. By denoting the poles as  $\{\hat{p}_{i,k}^0\}$ , the estimated ST and FT offsets are solved as

$$\hat{\mu}_i = \left\lfloor \frac{\angle \hat{p}_{i,k}^0}{-j2\pi f_0 T_f} \right\rfloor - i N_f - k, \quad (19)$$

$$\text{and } \hat{\nu}_i = \left\lfloor \frac{\angle \hat{p}_{i,k}^0}{-j2\pi f_0 T_s} \right\rfloor - Q (i N_f + k + \hat{\mu}_i), \quad (20)$$

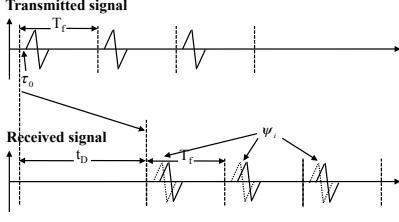


Figure 1: A pulse-based Terahertz signal model, with  $I = 1$  and  $N_f = 3$ .

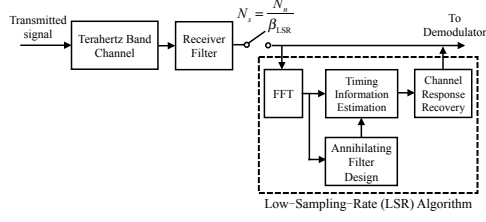


Figure 2: Block diagram of the LSR algorithm.

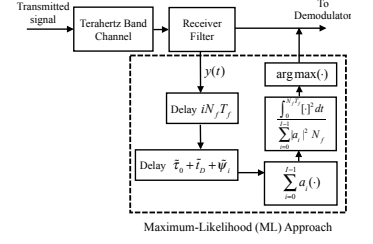


Figure 3: Block diagram of the ML approach.

where  $\lfloor \cdot \rfloor$  denotes the flooring operator.

This algorithm is reliable when the noise level is low and the antenna gains are high. In THz band communications, the use of very high gain antenna or antenna arrays can effectively improve the signal-to-noise ratio (SNR) and hence eliminate the noise effect. Nevertheless, the problem of numerical ill-conditioning may arise by using this approach, mainly because root-finding is not robust to noise. Instead of finding the roots, the matrix manipulations can be performed by exploiting the properties of the signal subspace [10]. However, a major computational cost of the above method arises in the singular value decomposition procedure in the matrix manipulation, which is an iterative algorithm with very high computational costs and is not favored in our work. In addition to the LSR algorithm, in the sequel section we propose an alternative solution to exploit the ML principle.

#### 4. MAXIMUM-LIKELIHOOD-BASED TIMING ACQUISITION APPROACH

In this section, the ML optimality criterion is adopted to derive a timing acquisition algorithm tailored to the pulse-based THz band communication. To start with the THz communication model (4), we denote the trial values of the unknown timing offsets as  $(\tilde{\tau}_0, \tilde{t}_D, \tilde{\psi}_i)^T$  and the channel-dependent received signal  $\tilde{g}(t)$ , which correspond to the parameters in (5) and (6). We consider the absence of intersymbol interference in the directional transmission, and treat the noise component  $w$  in the received signal (4) as a zero-mean Gaussian process over the receiver-filter bandwidth. Moreover, we describe  $\tilde{z}(t)$  as the noise-free component of the trial received signal, as

$$\tilde{z}(t) = \sum_{i=0}^{I-1} a_i \sum_{k=0}^{N_f-1} \tilde{g}(t - iN_f T_f - kT_f - \tilde{\tau}_0 - \tilde{t}_D - \tilde{\psi}_i). \quad (21)$$

We define  $\tilde{g}_1(t) = \sum_{k=0}^{N_f-1} \tilde{g}(t - kT_f)$ . The ML rule boils down to searching  $(\tilde{\tau}_0, \tilde{t}_D, \tilde{\psi}_i)^T$  and  $\tilde{g}_1(t)$  for the minimum of  $\|y(t) - \tilde{z}(t)\|^2$ , which equivalently maximizes

$$\begin{aligned} \Lambda \left[ y(t) \mid (\tilde{\tau}_0, \tilde{t}_D, \tilde{\psi}_i)^T, \tilde{g}_1(t) \right] &= 2 \int_0^{IN_f T_f} y(t) \tilde{z}(t) dt - \int_0^{IN_f T_f} [\tilde{z}(t)]^2 dt \\ &= 2 \int_0^{IN_f T_f} y(t) \sum_{i=0}^{I-1} a_i \tilde{g}_1(t - iN_f T_f - \tilde{\tau}_0 - \tilde{t}_D - \tilde{\psi}_i) dt \end{aligned}$$

$$- \int_0^{IN_f T_f} \left[ \sum_{i=0}^{I-1} a_i \tilde{g}_1(t - iN_f T_f - \tilde{\tau}_0 - \tilde{t}_D - \tilde{\psi}_i) \right]^2 dt \quad (22)$$

In this objective function, we assume that the training symbols  $a_i$  are uncorrelated with each other. Moreover, we recognize that one symbol waveform is confined with the non-zero support over  $[0, N_f T_f]$ . Hence, the objective function can be further arranged as

$$\begin{aligned} \Lambda \left[ y(t) \mid (\tilde{\tau}_0, \tilde{t}_D, \tilde{\psi}_i)^T, \tilde{g}_1(t) \right] &\approx 2 \sum_{i=0}^{I-1} a_i \int_0^{N_f T_f} \tilde{g}_1(t) \\ &\cdot y(t + iN_f T_f + \tilde{\tau}_0 + \tilde{t}_D + \tilde{\psi}_i) dt - \sum_{i=0}^{I-1} |a_i|^2 \int_0^{N_f T_f} [\tilde{g}_1(t)]^2 dt. \end{aligned} \quad (23)$$

This ML-based time acquisition problem can be solved by adopting a two-step procedure. In particular, the objective function can be rearranged by taking  $\tilde{g}_1(t)$  as the nuisance parameter, as

$$\begin{aligned} &(\tilde{\tau}_0, \tilde{t}_D, \tilde{\psi}_i)^T \\ &= \arg \max_{\tilde{g}_1(t)} \left\{ \max_{(\tilde{\tau}_0, \tilde{t}_D, \tilde{\psi}_i)^T} \left\{ \Lambda \left[ y(t) \mid (\tilde{\tau}_0, \tilde{t}_D, \tilde{\psi}_i)^T, \tilde{g}_1(t) \right] \right\} \right\}. \end{aligned} \quad (24)$$

To solve the inner term in (24), we fix  $(\tilde{\tau}_0, \tilde{t}_D, \tilde{\psi}_i)^T$  and set  $\frac{\partial \Lambda}{\partial \tilde{g}_1(t)} = 0$  in (23). The resulting optimal estimate of the received pulse waveform  $\tilde{g}_1(t)$  is obtained as

$$\tilde{g}_1(t) = \frac{1}{\sum_{i=0}^{I-1} |a_i|^2 N_f} \cdot \sum_{i=0}^{I-1} a_i y(t + iN_f T_f + \tilde{\tau}_0 + \tilde{t}_D + \tilde{\psi}_i). \quad (25)$$

This estimate can be interpreted as a weighted average template with the known training symbols  $a_i / \sum_{i=0}^{I-1} |a_i|^2$  as the weighting coefficients. By substituting (25) into (23) and (24), we reach the solution to the timing acquisition problem by using the two-step ML-based approach. The timing information is obtained as

$$\begin{aligned} &(\tilde{\tau}_0, \tilde{t}_D, \tilde{\psi}_i)^T = \arg \max \left\{ \frac{1}{\sum_{i=0}^{I-1} |a_i|^2 N_f} \right. \\ &\left. \int_0^{N_f T_f} \left[ \sum_{i=0}^{I-1} a_i y(t + iN_f T_f + \tilde{\tau}_0 + \tilde{t}_D + \tilde{\psi}_i) \right]^2 dt \right\}. \end{aligned} \quad (26)$$

The desired estimate is claimed when the received signal energy is maximized. The block diagram to implement the ML approach is illustrated in Fig. 3. The major cost of the ML

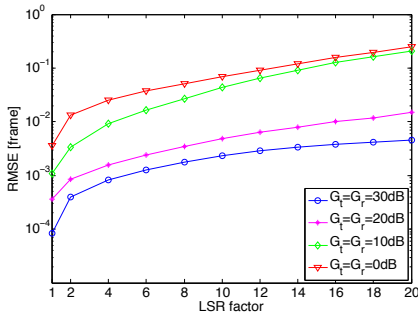


Figure 4: RMSE of LSR algorithm for different antenna gains.

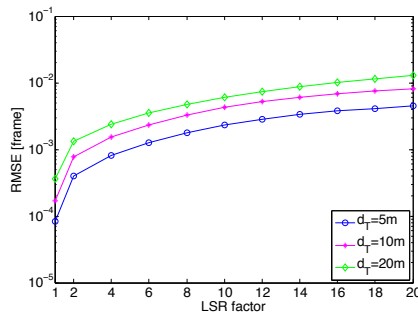


Figure 5: RMSE of LSR algorithm for different distances.

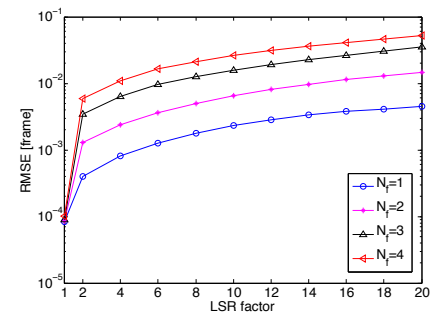


Figure 6: RMSE of LSR algorithm for different training symbols.

approach is the searching space, which can be reduced by enlarging the time step, at a multiple of  $T_s$ . Moreover, the storage of a large set of trail values is costly. The tradeoff between the synchronization performance and the complexity is investigated numerically in the next section.

## 5. PERFORMANCE EVALUATION

In this section, we evaluate the LSR synchronization algorithm and the ML-based approach in terms of the timing offset estimation performance, based on Monte Carlo simulations. Moreover, we study its influence on resulting received signals. All results are presented as the averages over 1000 iterations.

We consider the parameters in the simulations as follows. The random initial delay  $\tau_0$  and the random misalignment between the transmitter and the receiver  $\psi_i$  in (6) follow uniform distributions over  $[-T_f, T_f]$ , at the multiples of  $T_s = 0.5\text{ps}$ . In terms of the signal model in Sec. 2.2, the pulse width  $T_p = 10\text{ps}$ , the frame length  $T_f = 1\text{ns}$ , the frequency step  $f_0 = 10\text{MHz}$ . Moreover, for the THz band communication, the transmit power is  $S_t = 1\text{dBm}$ , the noise power is  $P_w = -80\text{dBm}$ , and the distance is  $d_T = 5\text{m}$  [7].

### 5.1 LSR Algorithm Performance

We study the RMSE for different combinations of LSR factors, antenna gains, transmission modes, and distances. As our main objective is to achieve an accurate synchronization by using a sub-Nyquist sampling rate, we investigate the LSR factor  $\beta_{\text{LSR}}$  that can support  $\text{RMSE} \leq 0.01T_f$ . The results are detailed as follows.

In Fig. 4, the RMSE performance over different antenna gains are evaluated. In particular, when the antenna gains  $G_t = G_r = 30\text{dB}$  and the communication distance  $d_T = 5\text{m}$  in (1),  $\beta_{\text{LSR}} = 20$  can be adopted. In this case, the path loss is approximately 117 dB and the resulting signal-to-noise ratio (SNR) is equal to 20 dB. On the one hand, the reduction of antenna gains implies to decrease SNR, which makes RMSE to increase significantly. As the antenna gains are equal to 20 dB, 10 dB and 0 dB, the maximum LSR factor reduces from 16 to 4 and 2. Hence, when the antenna gains or the equivalent SNR are very small, the RMSE becomes significant and the LSR algorithm is not suitable to be used. Moreover, we study the influence of communication distances on the synchronization performance, in Fig. 5. In general, as the distance increases, higher path loss and more severe frequency-selectivity appear in the THz band spectrum. This consequently degrades the RMSE of the LSR

algorithm. Although the LSR factor 20 can be supported to achieve  $\text{RMSE} = 0.01$  frame, the average RMSE values reduce from 0.003, 0.005, 0.007 to 0.011, as the distance increases from 5m, 10m, to 20m.

In addition, different numbers of the pulses to represent one training symbol are compared in Fig. 6. The worst RMSE occurs when each symbol consists of 4 repeated pulses. This can be understood that with additional repeated pulses in one symbol, the fluctuation of the frequency response becomes more severe. This results in the worse performance of the LSR algorithm as the low sampling rate is used to recover the received signal. For example, when  $N_f = 4$ , the LSR algorithm is proper to be used if the LSR factor needs to stay below 4. Furthermore, five pulses with the different supporting bandwidth are compared in Fig. 7. With the very small pulse duration,  $T_p$ , the supporting bandwidth is large. By using the LSR algorithm in the frequency domain, the wider frequency response yields better performance. In particular, a 10ps pulse has the frequency response occupying the 0.06-1 THz. This pulse waveform is able to support the  $\text{RMSE} = 0.01$  frame with the LSR factor of 20. In contrast, this LSR factor decreases as the pulse width in the frequency domain decreases. When a 20 GHz pulse is used, the largest LSR factor to satisfy the RMSE constraint reduces to 16.

### 5.2 Influence on Received Signals

We analyze the effect of the LSR on the received signal for different LSR factors, in Fig. 8. With smaller sampling rates, the recovery of received signals becomes more challenging. To compare the received signals sampled at sub-Nyquist rates with the original pulse, the RMSE of the received signal (not the timing acquisition) increases from  $1.26 \times 10^{-3}$ ,  $2.33 \times 10^{-3}$  to  $4.50 \times 10^{-3}$ , when  $\beta_{\text{LSR}} = 6, 10$  and 20. In addition to the amplitude and phase distortion, temporal broadening effects appear, due to the very high frequency-selectivity in the wideband THz spectrum [2]. The width of the received pulse with  $\beta_{\text{LSR}} = 1$  is over 200ps, which is 20 times larger than the transmitted pulse. However, by using a low sampling rate, the rapid fluctuation in the received pulses dwindles, and hence, the broadening effects attenuate. For example, when the LSR factors are 10 and 20, the width of the received pulse reduces to 180ps and 150ps, respectively. These are equivalent to suggest the maximal pulse rates of 5.56 and 6.67 Giga-pulses-per-second to avoid the inter-symbol-interference. Hence, LSR can effectively relax the restriction of the minimum spacing between consecutive pulses and hence, can improve the data rates.

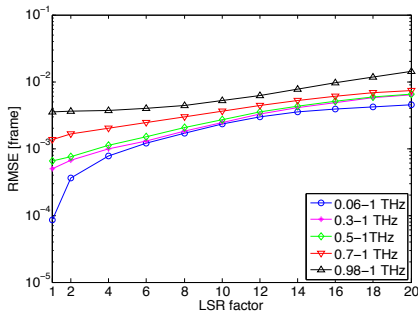


Figure 7: RMSE of LSR algorithm for different frequency bands.

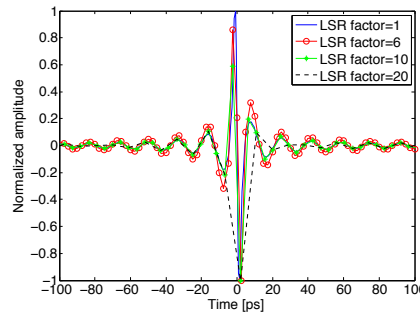


Figure 8: Sampled signals for different LSR factors.

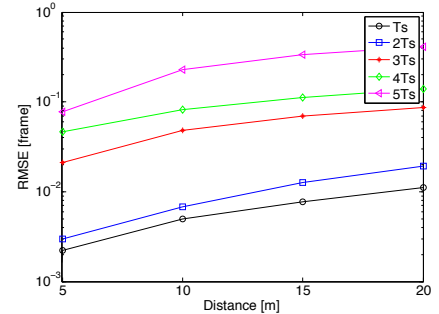


Figure 9: RMSE of ML approach for different time step.

### 5.3 ML Approach Performance

The LSR algorithm is not favored when the SNR at the receiver is low or equivalently in the multipath propagation. As an alternative, the ML approach yields better performance than the LSR algorithm, at the cost of significant searching space and data storage. The RMSE performance of the ML-based approach is analyzed in Fig. 9. As a major computation constraint, different time step values (at the multiples of  $T_s$ ) of the trial values in (26) are studied. The RMSE increases when the distance increases and the searching space decreases. To achieve RMSE = 0.01 frame, a time step of  $2T_s$  can be used to reduce the search space by half. However, the distances needs to remain below 15m. Specifically at  $d_T = 5\text{m}$ , the RMSE increases from 0.002, 0.003, 0.021, 0.046 to 0.077 when the time step increases from 1 to 5, respectively. Hence, the ML-based algorithm can be used in the multipath propagation with a time step of 2 to reduce the searching space by half.

## 6. CONCLUSION

In this paper, we proposed a LSR algorithm and a ML-based algorithms for timing acquisition in the THz band to address the challenges such as the ultra-high sampling rate demand, the stringent timing requirement for demodulation, and the THz band communication peculiarities. These two algorithm are evaluated based on the RMSE performance. The simulation results showed that in the directional transmission, the LSR algorithm can be used with the uniform sampling at  $1/20$  of the Nyquist rate, while the ML-based algorithm can be used in the multipath propagation with a time step of 2 to reduce the searching space by half. This analysis contributes to achieving the reliable timing acquisition with low computational complexity in the THz band.

## 7. ACKNOWLEDGEMENT

This work was supported by the U.S. National Science Foundation (NSF) under Grant No. CCF-1349828 and in part by Alexander von Humboldt Foundation through Dr. Ian F. Akyildiz's Humboldt Research Prize in Germany.

## 8. REFERENCES

- [1] S. R. Aedudodla, S. Vijayakumaran, and T. F. Wong. Timing acquisition in ultra-wideband communication systems. *IEEE Transactions on Vehicular Technology*, 54(5):1570–1583, 2005.
- [2] I. F. Akyildiz, J. M. Jornet, and C. Han. Terahertz Band: Next Frontier for Wireless Communications. *Physical Communication (Elsevier) Journal*, 12:16–32, 2014.
- [3] R. G. Baraniuk, E. Candès, R. Nowak, and M. Vetterli. Compressive sampling. *IEEE Signal Processing Magazine*, 25(2):12–13, 2008.
- [4] C. Han, A. O. Bicen, and I. F. Akyildiz. Multi-Ray Channel Modeling and Wideband Characterization for Wireless Communications in the Terahertz Band. *IEEE Transactions on Wireless Communications*, 14(5):2402–2412, 2015.
- [5] J. M. Jornet, and I. F. Akyildiz. Channel Modeling and Capacity Analysis for Electromagnetic Wireless Nanonetworks in the Terahertz Band. *IEEE Transactions on Wireless Communications*, 10(10):3211–3221, 2011.
- [6] J. M. Jornet and I. F. Akyildiz. Femtosecond-long pulse-based modulation for terahertz band communication in nanonetworks. *IEEE Transactions on Communications*, 62(5):1742–1754, 2014.
- [7] T. Kleine-Ostmann and T. Nagatsuma. A Review on Terahertz Communications Research. *Journal of Infrared, Millimeter and Terahertz Waves*, 32:143–171, 2011.
- [8] J. Kusuma, A. Ridolfi, and M. Vetterli. Sampling of communication systems with bandwidth expansion. In *Proc. IEEE International Conference on Communications (ICC)*, volume 3, pages 1601–1605, 2002.
- [9] J. Y. Lee and R. A. Scholtz. Ranging in a dense multipath environment using an uwb radio link. *IEEE Journal on Selected Areas in Communications (JSAC)*, 20(9):1677–1683, Dec. 2002.
- [10] I. Maravic and M. Vetterli. Sampling and reconstruction of signals with finite rate of innovation in the presence of noise. *IEEE Transactions on Signal Processing*, 53(8):2788–2805, 2005.
- [11] H. Song and T. Nagatsuma. Present and Future of Terahertz Communications. *IEEE Transactions on Terahertz Science and Technology*, 1(1):256–263, 2011.
- [12] M. Vetterli, P. Marziliano, and T. Blu. Sampling signals with finite rate of innovation. *IEEE Transactions on Signal Processing*, 50(6):1417–1428, 2002.